PRAMANA
— journal of
physics

Vol. 66, No. 6
June 2006
pp. 985–997

Effect of entrance channel parameters on the fusion of two heavy ions: Excitation functions of reaction products in ^{16}O + ^{66}Zn and ^{37}Cl + ^{45}Sc reactions

SUPARNA SODAYE, B S TOMAR and A GOSWAMI*
Radiochemistry Division, Bhabha Atomic Research Centre, Mumbai 400 085, India
*Corresponding author. E-mail: agoswami@barc.gov.in

MS received 27 December 2005; revised 15 February 2006; accepted 15 April 2006

Abstract. Excitation functions of reaction products formed in ^{16}O + ^{66}Zn and ^{37}Cl + ^{45}Sc systems, leading to the same compound nucleus, ^{82}Sr, were measured using recoil-catcher technique and off-line γ-ray spectrometry. The contribution of non-compound processes like transfer and incomplete fusion (ICF) reactions to the cross-sections of different evaporation residues were delineated by comparing the experimental data with the predictions of Monte Carlo simulation code PACE2. The results show that non-compound processes become a significant fraction of the total reaction cross-section in ^{16}O + ^{66}Zn systems in the beam energy range studied, while ^{37}Cl + ^{45}Sc gives mainly compound nucleus products. The mass asymmetry dependence of the fusion and non-compound cross-sections have been analysed in terms of the static fusion model and sum rule model.

Keywords. Nuclear reactions; incomplete fusion reactions; transfer reactions; non-compound nucleus processes; ^{16}O, ^{37}Cl beams; ^{66}Zn, ^{45}Sc targets; γ-ray spectrometry.

PACS Nos 25.70.Gh; 25.70.Jj

1. Introduction

The mechanism of fusion of two heavy ions has been extensively investigated [1–4]. The motivation for such studies is to understand the effect of entrance channel parameters, viz., energy, angular momentum and mass asymmetry, on the fusion process. In the static fusion model, fusion process is viewed as the problem of crossing the barrier in the one-dimensional interaction potential between the two heavy ions [3,4]. A large body of data on fusion cross-sections, spanning wide range of target–projectile combinations and energy, has been explained on the basis of this model. The occurrence of deep inelastic collisions (DIC) in heavy-ion reactions has led to the development of dynamical model [1,5–8], which describes DIC as well as fusion in a unified way. In a simplistic approach, classical equations of motion involving macroscopic variables R, the distance of approach of the two heavy ions

and θ, the polar angle between the direction of this composite system and the direction of the incident beam, are solved. Radial and tangential frictional forces are introduced in the equations of motion to take into account the dissipation of relative kinetic energy and angular momentum into internal degrees of freedom of the composite system. In this model, two heavy ions fuse if (i) there is a pocket in the entrance channel one-dimensional interaction potential and (ii) a given trajectory (solution of the equations of motion) ends up into the pocket of the entrance channel potential. If the l-wave is not trapped in the pocket, the two ions re-separate loosing much of their relative kinetic energy and angular momentum and gives rise to deep inelastic collision.

However, identification of the fusion process with trapping of the composite system into the potential pocket become uncertain, when heavier projectiles are used and at higher bombarding energies. Even after being trapped, the composite system may evolve towards symmetric fragmentation, without forming a true compound nucleus (CN) [9]. Study of entrance channel energy and mass asymmetry dependence of the reaction mechanism, therefore, remains an interesting area of research [10–15].

In this paper, we report the excitation functions for the heavy residues formed in the ^{16}O + ^{66}Zn and ^{37}Cl + ^{45}Sc reactions, forming the same compound nucleus, ^{82}Sr. The experimental results have been compared with the statistical model calculations using PACE2 code to identify the channels arising from the non-compound processes like transfer and incomplete fusion (ICF) reactions. Variation of the cross-sections of the non-compound processes over a range of beam energy, for both the systems, has been investigated. The mass asymmetry dependence of the fusion and non-compound cross-sections have been analysed in terms of the static fusion and sum rule model.

2. Experimental details

The experiments were carried out at BARC-TIFR pelletron facility at Mumbai. For ^{16}O + ^{66}Zn system, self-supporting metal foils of 99.5% enriched ^{66}Zn (thickness 2.5 mg/cm^2), were irradiated with ^{16}O beam. A short (5 min) and a long (60 min) irradiation were carried out at each of the beam energies. Measurements were carried out at seven beam energies in the range of 61–93 MeV. The recoiling products were collected on aluminium catcher foils of thickness 2 mg/cm^2. For ^{37}Cl + ^{45}Sc system, self-supporting scandium metal foils of thickness 400–700 μg/cm^2 were bombarded with ^{37}Cl beam in the beam energy range of 100–124 MeV. Depending on the beam current, the irradiation time was 2–4 h. The thickness of the scandium target foils was measured by alpha energy loss method using a ^{241}Am source and the stopping power table of Northcliffe and Schilling [16]. The error on the thickness of the targets was around 5%, owing to the uncertainty in defining the peak energy in the alpha spectrum. Gold foil of 10 mg/cm^2 thickness was used to stop all the recoiling evaporation residues formed in the ^{37}Cl + ^{45}Sc reaction as TRIM code calculations showed that the recoiling CF products, formed in 124 MeV ^{37}Cl beam-induced reaction on scandium target, have a range of $\sim$6.6 mg/cm^2 in gold. The beam energy range of ^{37}Cl used in the present investigations was below

the Coulomb barrier ($V_{\rm C}$) for ^{197}Au and, therefore, there was no interference from the ^{37}Cl + ^{197}Au reactions.

In both the systems, the products were assayed by off-line γ-ray spectrometry using a HPGe detector coupled to a PC-based 4k channel analyser (MCA). The target and the catcher foil were counted together for γ-ray activity of ERs. The counting was followed for two weeks in both the cases. The γ-ray spectra were analysed using the peak fitting software *Phast* [17] with peak shape having the form of a Gaussian function with lower exponential tail and polynomial background.

The measured peak areas were corrected for counting time to get count rate CR($T_{\rm c}$) as a function of cooling time ($T_{\rm c}$). From the measured CR($T_{\rm c}$), the cross-sections (σ) for the reaction products were calculated using the standard relation

$$\mathrm{CR}(T_{\rm c}) = N\sigma\phi(1-\mathrm{e}^{-\lambda T_i})\mathrm{e}^{-\lambda T_{\rm c}} I_\gamma \varepsilon_\gamma, \tag{1}$$

where N is the number of target atoms/cm^2, ϕ is the number of beam particles falling on the target per unit time as measured by an electron suppressed Faraday cup placed behind the target catcher assembly, λ is the decay constant of the radionuclide of interest, T_i is the duration of irradiation, I_γ and ε_γ are respectively the intensity and detection efficiency of the γ-ray of interest. For measuring the beam intensity from the charge collected on the Faraday cup, information about the charge state of the energetic heavy ions is important. The selected charge state of the energetic heavy ions might get modified when they traverse through the target foils. The average charge state of the ions emerging from the target catcher assembly was calculated using the Schiwietz [18] formalism. According to this formalism, the charge of an ion (atomic number $z_{\rm p}$) emerging from a target (atomic number $z_{\rm t}$) with a velocity $v_{\rm p}$ is given by

$$\overline{q_{\rm mean}} = z_{\rm p}\left\{\frac{12x+x^4}{(0.07/x)+6+0.3x^{0.5}+10.37x+x^4}\right\},$$

where

$$x = \left(\frac{v_{\rm p}}{1.68v_0} z_{\rm p}^{-0.52} z_{\rm t}^{-0.019\frac{v_{\rm p}}{v_0} z_{\rm p}^{-0.52}}\right)^{1+\frac{1.8}{z_{\rm p}}}.$$

v_0 is the Bohr's velocity and has the value 2.19×10^6 m/s. The detection efficiency (ε_γ) was obtained by counting a calibrated ^{152}Eu source in the same geometry. Table 1 gives the spectroscopic data [19] used in the present studies.

The cross-sections of the two ^{78}Rb isomers, ^{78}Rb$^{\rm m}$ (4^-) and ^{78}Rb$^{\rm g}$ (0^+) were deduced by fitting the common γ-line of 455 keV into two independently decaying radionuclides. The 10% IT decay of ^{78}Rb$^{\rm m}$ to ^{78}Rb$^{\rm g}$ was neglected. In the case of ^{77}Br, the high-spin isomer ^{77}Br$^{\rm m}$ ($9/2^+$) decays by IT (100%) to ground state ^{77}Br$^{\rm g}$ ($3/2^-$) and hence the cross-section of ^{77}Br$^{\rm g}$ represents the sum of the cross-sections of both the isomers. Similarly, the cross-section of ^{76}Br$^{\rm g}$ represents the sum of cross-sections of both the isomers due to >99% IT decay of short-lived ^{76}Br$^{\rm m}$ (4^+) to ^{76}Br$^{\rm g}$ (1^-). In some cases, the cross-section of the high-spin isomer only could be measured, e.g. ^{73}Se (2n product). In such cases, the cross-section of the high-spin isomer was considered to represent the cross-section of the radionuclide. This is a good approximation as more than 90% of the cross-section appears in

Table 1. Spectroscopic data used in the present studies.

Radionuclide	Half-life	E_γ (keV)	I_γ (%)
^{79}Rb	22.9 min	182.8	19.2
^{78}Rb^{m}	5.74 min	455.0	81.0
^{78}Rb^{g}	17.66 min	455.0	62.5
^{79}Kr	35.04 h	261.3	12.7
^{77}Kr	1.24 h	129.7	81.0
^{76}Kr	14.8 h	315.7	39.0
^{77}Br^{g}	2.38 d	520.7	22.4
^{76}Br	16.2 h	559.1	74.0
^{75}Br	1.62 h	286.5	88.0
^{73}Se^{g}	7.15 h	361.2	108.2
^{47}Sc	3.93 h	1157.1	99.9
^{44}Sc^{g}	3.34 d	159.4	68.0
^{48}V	15.97 d	983.5	100.0
^{69}Ge	39.05 h	1106.8	36.0
^{67}Ge	18.7 min	167.0	84.3
^{67}Ga	78.3 h	184.6	21.2
^{66}Ga	9.4 h	1039.3	37.0

the high-spin isomer due to the high angular momentum involved in the heavy-ion reactions. In the case of ^{44}Sc, the peak area of the common γ-line (1157 keV) of both the isomers of ^{44}Sc was found to follow the half-life of the low-spin ^{44}Sc$^{g}(2^{+})$ and hence the 1157 keV γ-line was used to evaluate the cross-section of ^{44}Sc^{g}.

3. Results and discussion

Excitation functions of 13 reaction products in the case of ^{16}O + ^{66}Zn system and 12 reaction products in the case of ^{37}Cl + ^{45}Sc system were measured. Figures 1a–e and 2a–e show the excitation functions of different products formed in ^{16}O + ^{66}Zn and ^{37}Cl + ^{45}Sc systems respectively. Errors in the measurement of detection efficiency, target thickness and counting statistics result in around 10–15% error on the experimental data.

The theoretical excitation functions of evaporation residues were obtained using the Monte Carlo simulation code PACE2 [20]. The KRK level density prescription [21] was used which takes into account the excitation energy dependence of the level density. The optical model parameters of Perey and Perey [22] were used for the emitted alphas, protons and neutrons. The average gamma transition strengths compiled by Endt [23] were used in the present work. For the excitation function calculations, the value of level density parameter a was taken as $A/8$. The other input parameters in the programme were used as default values. The calculated excitation functions are shown as broken lines in figures 1 and 2.

Both ^{16}O + ^{66}Zn and ^{37}Cl + ^{45}Sc reaction systems lead to formation of the same compound nucleus, ^{82}Sr. Figure 3 gives the excitation energy dependence of the

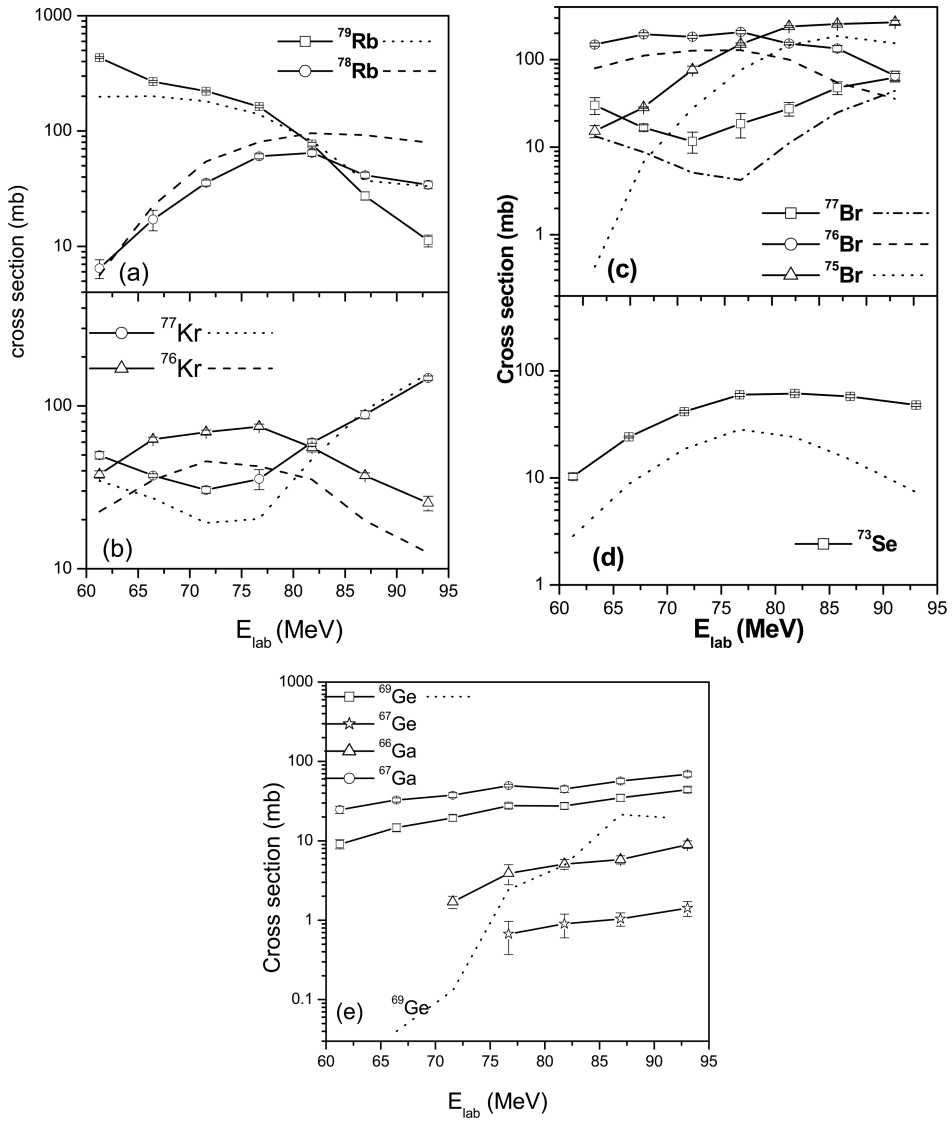

Figure 1. Excitation functions of reaction products formed in ^{16}O + ^{66}Zn system. The broken lines are the respective PACE2 calculations.

experimental cross-section of one of the evaporation residue, ^{79}Kr, produced in both the systems. The cross-section is represented as the fraction of total fusion cross-section ($\sigma_{\rm CN}$), which was obtained from PACE2 calculations. Since the precursor ^{79}Rb also decays to ^{79}Kr and has a much smaller half-life (table 1), the ^{79}Kr cross-section represents the total (^{79}Rb + ^{79}Kr) cross-section. The cumulative cross-section of ^{79}Kr was plotted because it is expected to originate from compound nucleus process only. As expected from the compound nucleus hypothesis, the two

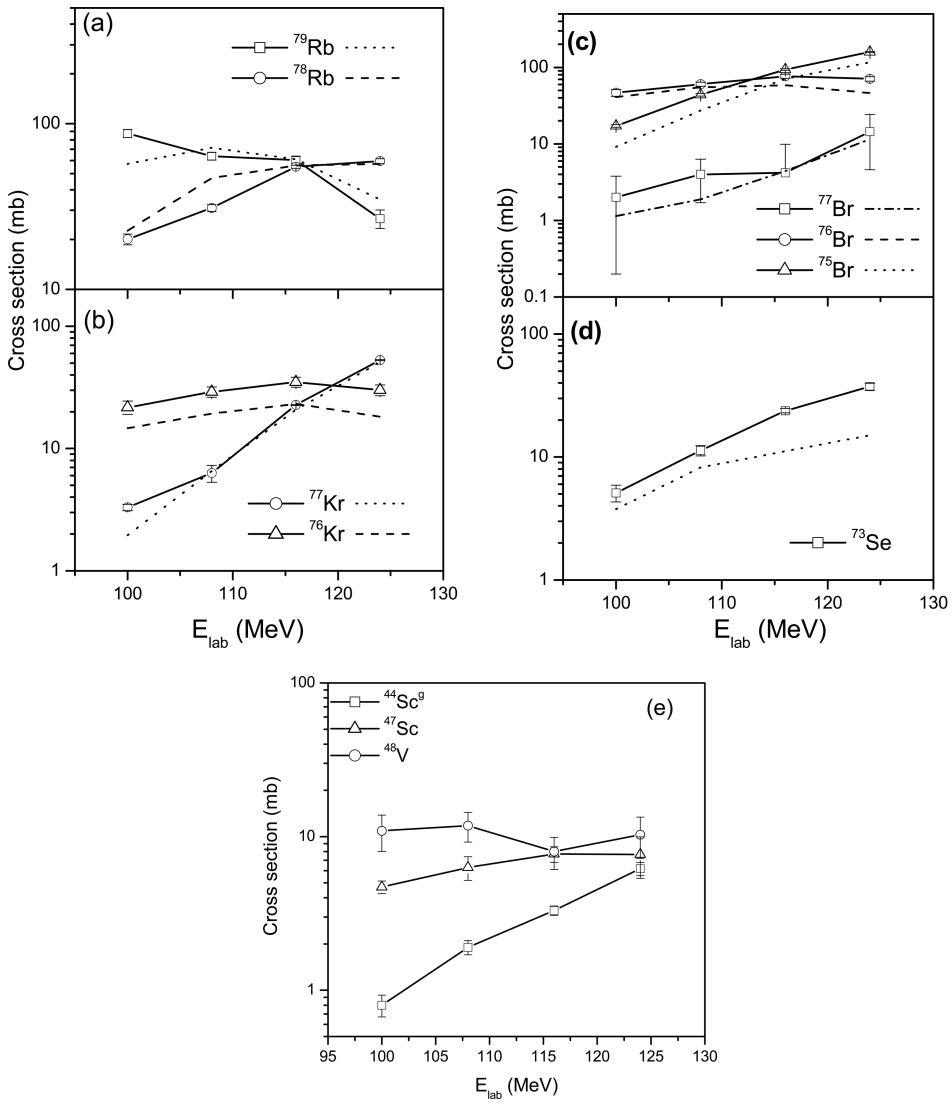

Figure 2. Excitation functions of reaction products formed in ^{37}Cl + ^{45}Sc system. The broken lines are the respective PACE2 calculations.

fractional cross-sections match well for both the systems, indicating matching E^* and l-distribution over the beam energy range used. The agreement also shows the validity of the procedure used for charge state correction in both the systems. The data are compared with the same obtained from PACE2 calculations. Close agreement between the experimental and calculated values shows that parameters used for the PACE2 calculations are reasonably accurate.

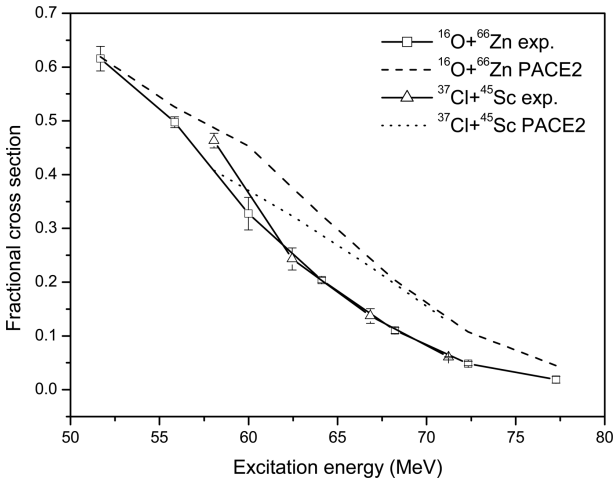

Figure 3. Excitation energy dependence of the cross-section of ^{79}Kr isotopes produced in ^{16}O + ^{66}Zn and ^{37}Cl + ^{45}Sc systems. The cross-section is represented as the fraction of total fusion cross-section ($\sigma_{\rm CN}$), which was obtained from PACE2 calculations.

Comparison of the experimental excitation functions with the theoretically calculated excitation functions of the proton emission (pxn) products, namely, ^{79}Rb and ^{78}Rb, revealed that the experimental cross-sections agree well with the calculated cross-sections in both the systems (figures 1a and 2a), indicating that these ERs are formed purely by complete fusion of projectile and target.

The experimental cross-sections of αn emission channel (^{77}Kr) deviate from the calculated cross-section in the case of ^{16}O + ^{66}Zn (figure 1b) while it is well-reproduced in the case of ^{37}Cl + ^{45}Sc (figure 2b) system. The experimental cross-sections of $\alpha 2n$ emission product (^{76}Kr) are significantly higher than the calculated values in ^{16}O + ^{66}Zn (figure 1b) while they are slightly higher in the case of ^{37}Cl + ^{45}Sc (figure 2b) system. The experimental cross-sections of the αpxn products, ^{77}Br, ^{76}Br and ^{75}Br, are found to be higher than the calculated ones in the case of ^{16}O + ^{66}Zn (figure 1c) system whereas they are close to the calculated ones in the case of ^{37}Cl + ^{45}Sc (figure 2c) system.

In the case of ^{73}Se, which is a $2\alpha n$ product, the experimental cross-sections are higher than the calculated cross-section in both the systems, though the difference is more pronounced in ^{16}O + ^{66}Zn system (figures 1d and 2d). The germanium and gallium isotopes, namely, ^{69}Ge, ^{67}Ge, ^{67}Ga and ^{66}Ga may be formed in the direct transfer reactions in the ^{16}O + ^{66}Zn system (figure 1e). Similarly the target-like products, ^{48}V, ^{44}Sc$^{\rm g}$ and ^{47}Sc in the case of ^{37}Cl + ^{45}Sc system may be formed in the direct transfer reactions (figure 2e).

The mismatch in the experimental and calculated excitation functions has been considered to be due to contribution from non-compound processes in those channels. The excess cross-sections over what is expected from the compound nucleus process has been computed for each channel, at each beam energy, to obtain an estimate of the total non-compound cross-section as a function of beam energy for both

Table 2. Non-compound nucleus process cross-section and l_{max} for the two systems.

E_{beam} (MeV)	E^* (MeV)	σ_{CN} (mb) PACE2	l_{cr} ($\hbar$) PACE2	σ_{NCN} (mb)	l_{max} (exp.) ($\hbar$)	l_{max} (calc.) ($\hbar$)
$^{16}O + {}^{66}Zn$						
61	51.7	857	28.7	164±10	31±1	28.9
66	55.8	981	32.0	214±9	35±1	32.8
72	60.0	1079	34.9	228±11	38±2	36.9
76	64.1	1157	37.4	324±13	42±2	39.4
82	68.2	1219	39.6	304±11	44±2	42.9
87	72.3	1240	41.2	308±16	46±2	45.6
93	77.3	1255	42.9	319±19	48±2	48.7
$^{37}Cl + {}^{45}Sc$						
100	57.9	354	24.5	34±5	26±1	23.2
108	62.2	540	31.5	51±5	33±1	31.5
116	66.6	690	36.8	66±7	39±1	38.0
124	71.0	824	41.6	104±12	44±1	43.6

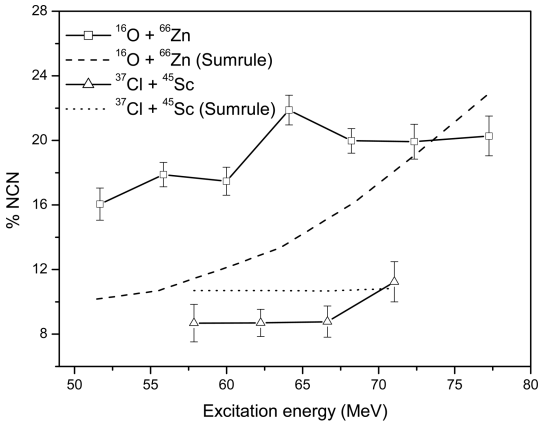

Figure 4. Percentage non-compound nucleus (NCN) processes in both the systems as a function of excitation energy. The lines are sum rule model predictions for $^{16}O + {}^{66}Zn$ (broken line) and $^{37}Cl + {}^{45}Sc$ (dotted line).

the systems (table 2). In both the cases, the cross-section for the transfer channels has also been included in the calculation of total non-compound cross-section.

Figure 4 gives the percentage of non-compound nucleus (NCN) processes as a function of excitation energy (E^*) of the compound nucleus for both the systems. While calculating the total reaction cross-section, the compound nucleus cross-section values were taken from the PACE2 code since all the evaporation residues could not be tagged experimentally. The uncertainty in the % NCN cross-section is the propagated error on the experimental cross-section. Additional uncertainty of

the order of 10–15% could be there because of the error in the PACE2 data, which is not shown in the figure. The NCN cross-sections (8–10%) for ^{37}Cl + ^{45}Sc system are less than the other system in the beam energy range studied. The % NCN cross-section gradually increases with beam energy for ^{16}O + ^{66}Zn system, whereas it remains practically invariant for ^{37}Cl + ^{45}Sc system in the beam energy range studied. This may be due to the fact that the transfer channels mainly contribute to NCN processes in ^{37}Cl + ^{45}Sc system, while for the ^{16}O + ^{66}Zn system, incomplete fusion (ICF) processes, in the form of α and 2α emission channels are observed. In incomplete fusion reactions, a part of the projectile fuses with the target nucleus, while the remaining fragment escapes in the forward direction with almost the beam velocity [24]. They are known to occur in reactions involving highly asymmetric target–projectile combination, and the mass flow is invariably from projectile to target [25]. The experimental values of $l_{\max}$ for both the systems, at each beam energy, were obtained from the reaction cross-section (σ_{R}) using the formula

$$l_{\max} = \sqrt{\frac{\sigma_{\mathrm{R}}}{\pi\lambda^2}} - 1,$$

where $\sigma_{\mathrm{R}} = \sigma_{\mathrm{CN}} + \sigma_{\mathrm{NCN}}$. The $l_{\max}$ values are also calculated using the formula

$$l_{\max} = \frac{(R_{\mathrm{p}} + R_{\mathrm{T}})\sqrt{2\mu(E_{\mathrm{CM}} - V_{\mathrm{C}})}}{\hbar}$$

and are given in table 2 along with the experimental values. The values of compound nucleus cross-section (σ_{CN}) and the corresponding critical angular momentum for fusion (l_{cr}) obtained from PACE2 calculations are also given in the table. It can be seen that there is a good agreement between the experimental and calculated values of $l_{\max}$. In the present context, the NCN processes mainly constitute transfer and ICF processes. While transfer reactions start occurring at beam energy around the Coulomb barrier, the ICF reactions are expected to occur at beam energies where the pocket in the entrance channel interaction potential disappears [25]. The total interaction potential for both the systems was calculated using the prescription given in ref. [4]. The total interaction potential $V(R)$ can be decomposed in a nuclear part, $V_{\mathrm{N}}(R)$, a Coulomb contribution $V_{\mathrm{C}}(R)$ and a centrifugal energy $V_{\mathrm{l}}(R)$ such that

$$V(R) = V_{\mathrm{N}}(R) + V_{\mathrm{C}}(R) + V_{\mathrm{l}}(R).$$

For not too small inter-nuclear distance $R > (A_1^{1/3} + A_2^{1/3})$,

$$V_{\mathrm{C}}(R) = \frac{Z_1 Z_2 e^2}{R},$$

$$V_{\mathrm{l}}(R) = \frac{l(l+1)\hbar^2}{2\mu R^2},$$

where μ is the reduced mass and

$$V_{\mathrm{N}}(R) = \frac{C_1 C_2}{C_1 + C_2} U_{\mathrm{N}}(s),$$

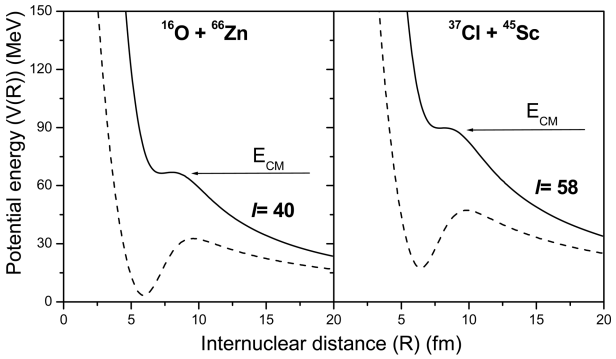

Figure 5. Calculated one-dimensional interaction potential for the two systems at $l = 0$ (dotted line) and the minimum l-value at which the pocket in the potential vanishes (solid line).

where

$$s = R - C_1 - C_2$$

and C_i is the half density radius given by

$$C_i = R_i - \frac{1}{R_i},$$

where $R_i (= 1.16A_i^{1/3})$ represents the sharp cut-off radius. $U_{\mathrm{N}}(s)$ can be parametrized by simple analytical formula

$$U_{\mathrm{N}}(s) = -34 \exp\left(-\frac{(s+1.6)^2}{5.4}\right) \quad \text{for } s > -1.6 \text{ fm},$$

and

$$U_{\mathrm{N}}(s) = -34 + 5.4(s+1.6)^2 \quad \text{for } s < -1.6 \text{ fm}.$$

Figure 5 shows the one-dimensional interaction potential for the two systems at $l = 0$ and minimum l value at which the pocket in the entrance channel interaction potential disappears. For ^{16}O + ^{66}Zn system, this pocket-vanishing l value is around 40–41 $\hbar$, at the corresponding beam energy of 82 MeV ($E^* = 68.4$ MeV). For ^{37}Cl + ^{45}Sc system the values are $l = 57$–58 $\hbar$ and $E_{\mathrm{beam}} \sim 160$ MeV ($E^* = 90.8$ MeV).

From the consideration of vanishing pocket in the interaction potential, ICF should have occurred in ^{16}O + ^{66}Zn system at around the highest beam energies studied in the present work. However, the data (figure 4) show that they compete with fusion process below the l-value corresponding to vanishing l-pocket. Our earlier work [26–28] and literature data [29–31] are consistent with this observation. For the ^{37}Cl + ^{45}Sc system, the highest beam energy studied in this work is well below the condition of vanishing l-pocket. This may be the reason why mainly transfer reactions are observed in this system.

So far, none of the proposed models on ICF give a quantitative estimate of the cross-sections of transfer/ICF reactions in heavy-ion reactions in the given excitation energy range. The sum rule model of Wilczynski *et al* [25], which takes into

account the transfer/break-up Q value for the calculation of cross-section for different channels, gives a semi-quantitative explanation of the NCN processes. We have compared our experimentally observed % NCN cross-sections with that estimated using the sum rule model calculations. The results are shown in figure 4. The sum rule model contains three free parameters, namely, R_c (the effective relative distance between the target and the projectile), Δ (diffuseness of the cut-off in the l-distribution) and T (the effective temperature). A variation of T as well as Δ changes the prediction of absolute cross-section of NCN channels, but the threshold energy for the occurrence of ICF process does not change much. The values used in the calculations were $R_c/(A_1^{1/3} + A_2^{1/3}) = 1.5$ fm and $\Delta = 1.7\hbar$ as used in the original sum rule model calculations of Wilczynski *et al* [25]. The other adjustable parameter T was taken as 4 MeV. A lower value of T highly underestimates the cross-sections in both the systems. As can be seen from figure 4, the sum rule model calculations give a reasonable agreement with the experimentally observed % NCN processes in the case of ^{37}Cl + ^{45}Sc system, where the l-values involved are much below the condition of vanishing pocket. This shows that, in this system, the products are a result of binary l-matched transfer reactions. For ^{16}O + ^{66}Zn system, the sum rule model calculations underestimate the % NCN cross-section for l-values below the condition of vanishing pocket, whereas it overestimates the cross-section for E^* beyond the vanishing l-pocket for the set of parameters used in the present calculations. There is not enough literature where sum rule model calculations have been used to produce the experimental NCN cross-section data over a wide range of E^* with a consistent set of adjustable parameters. To get a physical insight into the value of the adjustable parameters, particularly the effective temperature (T), a systematic analysis of a large amount of experimental data is further needed.

It would be interesting to see the effect of entrance channel mass asymmetry on the reaction mechanism in the present systems. According to Morgenstern systematics [32], there is a threshold for ICF reactions at $v_L/c = 0.06 \pm 0.02$, where v_L is the velocity of the lighter fragment and for the same v_{rel}/c, ICF cross-sections are more for a mass asymmetric system as compared to symmetric system. In the present case, this threshold corresponds to about 87 MeV for ^{16}O + ^{66}Zn system and 300 MeV for ^{37}Cl + ^{45}Sc system. As discussed above, the vanishing l-pocket condition predicts the threshold for ICF much lower than these energies and the experimental observation is that the threshold is still lower at least for the asymmetric ^{16}O + ^{66}Zn channel.

4. Conclusions

In the present work, the excitation functions of the reaction products formed in the two complementary entrance channels, namely, ^{16}O + ^{66}Zn and ^{37}Cl + ^{45}Sc, were measured by recoil catcher technique and off-line γ-ray spectrometry for beam energies above the Coulomb barrier. Comparison of the experimental excitation functions with the theoretically calculated values for CN de-excitation showed significant contribution of non-compound processes, viz., direct transfer and ICF, in the more asymmetric system (^{16}O + ^{66}Zn) than a more symmetric system

(^{37}Cl + ^{45}Sc) at comparable excitation energies. The analysis of the experimental fusion and non-compound cross-sections, in terms of the static fusion model as well as sum rule model, have revealed that the non-compound processes start competing with complete fusion processes at l-values much below the vanishing l-pocket for mass asymmetric entrance channel.

Acknowledgement

Authors thank Dr S B Manohar and Dr A V R Reddy, for their keen interest and encouragement during this work. The cooperation of the Pelletron operation crew during the experiment is gratefully acknowledged.

References

[1] M Lefort and C Ngô, *Ann. Phys. (Paris)* **3**, 5 (1978)
[2] P Armbruster, *Ann. Rev. Nucl. Part. Sci.* **35**, 135 (1985)
[3] J R Birkelund and J R Huizenga, *Ann. Rev. Nucl. Part. Sci.* **33**, 265 (1983)
[4] C Ngô, *Progress in particle and nuclear physics* edited by A Faessler (Pergamon, Oxford, 1985) vol. 16, p. 139
[5] N A Weidenmüller, *Progress in particle and nuclear physics* edited by D Wilkinson (Pergamon, Oxford, 1980) vol. 3
[6] C Ngô, *Approches phénoménologiques des collisions dissipatives entre ions lourds à basse énergie Note CEA-N-2354* (1983)
[7] W U Schröder and J R Huizenga, *Ann. Rev. Nucl. Sci.* **27**, 465 (1977); *Treatise on heavy ion science* edited by D A Bromley (Plenum, New York) vol. 2, chap. 3
[8] G Royer and B Remaud, *Nucl. Phys.* **A444**, 477 (1985)
[9] W J Swiatecki, *Phys. Scr.* **24**, 113 (1981)
[10] R Babinet, L G Moretto, J Galin, R Jared, J Moulton and S G Thompson, *Nucl. Phys.* **A258**, 172 (1976)
[11] S Agarwal, J Galin, B Gatty, D Guerreau, M Lefort, X Tarrago, R Babinet and J Girard, *Z. Phys.* **A296**, 287 (1980)
[12] V S Ramamurthy, S S Kapoor, R K Choudhury, A Saxena, D M Nadkarni, A K Mohanty, B K Nayak, S V Sastry, S Kailas, A Chatterjee, P Singh and A Navin, *Phys. Rev. Lett.* **65(1)**, 25 (1990)
[13] A C Berriman, D J Hinde, M Dasgupta, C R Morton, R D Butt and J O Newton, *Nature (London)* **413(13)**, 144 (2001)
[14] M Trotta, A M Stefanini, B R Behera, L Corradi, E Fioretto, A Gadea, S Szilner, Y W Wu, S Beghini, G Montagnoli, F Scarlassara, A Yu Chizhov, I M Itkis, G N Kniajeva, E M Kozulin, I V Pokrovsky, R N Sagaidak, V N Voskressensky, F Hass and N Rowley, *Prog. Theor. Phys., Suppl. No.* **154**, 37 (2004)
[15] C Beck, D G Kovar, S J Sanders, B D Wilkins, D J Henderson, R V F Janssens, W C Ma, M F Vineyard, T F Wang, C F Maguire, F W Prosser and G Rosner, *Phys. Rev.* **C39**, 2202 (1989)
[16] N C Northcliffe and R F Schilling, *At. Data Nucl. Data Tables* **A7**, 233 (1970)
[17] P Mukhopadhyaya, Private communication (2000)
[18] G Schiwietz and P L Grande, *Nucl. Instrum. Methods* **B175–177**, 125 (2001)

[19] R B Firestone and V S Shirley, *Table of isotopes*, 8th edition (John Wiley & Sons, New York, 1996)
[20] A Gavron, *Phys. Rev.* **C21**, 230 (1980)
[21] S K Kataria, V S Ramamoorthy and S S Kapoor, *Phys. Rev.* **C18**, 549 (1978)
[22] C M Perey and F G Perey, *At. Data Nucl. Data Tables* **17**, 1 (1976)
[23] P M Endt, *At. Data Nucl. Data Tables* **26**, 47 (1981)
[24] H C Britt and A R Quinton, *Phys. Rev.* **124**, 877 (1961)
[25] J Wilczynski, K Siwek-Wilczynska, J Van Driel, S Gongrijp, D C J M Hageman, R V F Janssens, J Lakasiak, R H Siemssen and S Y Vander Werf, *Nucl. Phys.* **A373**, 109 (1982)
[26] B S Tomar, A Goswami, A V R Reddy, S K Das, P P Burte, S B Manohar and Bency John, *Phys. Rev.* **C49**, 941 (1994)
[27] B Bindukumar, S Mukherjee, S Chakrabarty, B S Tomar, A Goswami and S B Manohar, *Phys. Rev.* **C57**, 743 (1998)
[28] S Chakrabarty, B S Tomar, A Goswami, G K Gubbi, S B Manohar, Anil Sharma, B Bindukumar and S Mukherjee, *Nucl. Phys.* **A678(4)**, 355 (2000)
[29] D J Parker, J Asher, T W Conlon and N Naquib, *Phys. Rev.* **C30**, 143 (1984)
[30] D J Parker, J J Hogan and J Asher, *Phys. Rev.* **C35**, 161 (1987)
[31] I Tserruya, V Steiner, Z Frankel, P Jacobs, D G Kovar, W Hennings, M F Vineyard and B G Glagola, *Phys. Rev. Lett.* **60**, 14 (1988)
[32] H Morgenstern, W Bohne, W Galster, K Grabisch and A Kyanowski, *Phys. Rev. Lett.* **52**, 1104 (1984)